ELSEVIER

Journal of Photochemistry and Photobiology A: Chemistry 141 (2001) 159–167

Journal of Photochemistry and Photobiology A:Chemistry

www.elsevier.nl/locate/jphotochem

Photochemistry of *fac*-$Pt(NO_2)_3Cl_3{}^{2-}$ complexes in water solutions

V.F. Plyusnin [a,*], E.M. Glebov [a], V.P. Grivin [a], Y.V. Ivanov [a], A.B. Venediktov [b], H. Lemmetyinen [c]

[a] *Institute of Chemical Kinetics and Combustion, 630090 Novosibirsk, Russia*
[b] *Institute of Inorganic Chemistry, 630090 Novosibirsk, Russia*
[c] *Institute of Materials Chemistry, Tampere University of Technology, PO Box 589, 33101 Tampere, Finland*

Received 20 February 2001; accepted 25 April 2001

Abstract

The photochemical transformation of *fac*-$Pt(NO_2)_3Cl_3{}^{2-}$ complex in water solutions and frozen matrices has been studied by laser flash photolysis, optical, ESR, and NMR spectroscopies. Upon steady-state photolysis of liquid water solutions, the *fac*-$Pt(NO_2)_3Cl_3{}^{2-}$ absorption bands disappear in the optical spectrum with both the preservation of isosbestic point at 43 620 cm^{-1} and the appearance of a new absorption band with a maximum at 48 000 cm^{-1}, belonging to Pt(II) complexes. Applying the NMR method to nuclei ^{195}Pt and ^{14}N, we have shown that the final photolysis products are mainly complexes $[PtCl_3(NO_2)]^{2-}$, $Pt(NO_2)_2(H_2O)_2$, and $[Pt(NO_2)_6]^{2-}$. The photolysis of frozen ($H_2O + LiCl$ or $H_2O + MgClO_4$) matrices containing the *fac*-$Pt(NO_2)_3Cl_3{}^{2-}$ complex yields a new wide absorption band with a maximum in a region of 30 000 cm^{-1} which belongs to the $[PtCl_3(NO_2)_2(ONO)]^{2-}$ nitrito-isomer of the initial complex. A longer irradiation causes photodissociation of nitrito-isomer into a complex of trivalent platinum $[PtCl_3(NO_2)_2]^{2-}$ and free $NO_2{}^{\bullet}$ radical whose characteristic lines are manifested in the ESR spectrum. The laser flash photolysis shows that in solution at room temperature, the $[PtCl_3(NO_2)_2(ONO)]^{2-}$ nitrito-isomer thermally dissociates in about 300 ns with an activation energy of 48.6 ± 1.7 kJ mol^{-1}. The $[PtCl_3(NO_2)_2]^{2-}$ complex dissociates in about 7 μs giving the second free $NO_2{}^{\bullet}$ radical and a $[PtCl_3(NO_2)]^{2-}$ complex. This reaction has an activation energy of 37.6 ± 1.5 kJ mol^{-1}. It is shown that dissociation of the $[PtCl_3(NO_2)_2]^{2-}$ complex is reversible and the $NO_2{}^{\bullet}$ radical coordinates again with the $[PtCl_3(NO_2)]^{2-}$ ion with a rate constant $4.2 \times 10^9\ M^{-1}\ s^{-1}$. In addition to the repeated coordination, the $NO_2{}^{\bullet}$ radical also disappears in a reversible reaction of recombination ($2k_{rec} = 1.8 \times 10^9\ M^{-1}\ s^{-1}$) to give N_2O_4 molecule.

Keywords: Mixed nitrito-chloride Pt(IV) complexes; Photochemistry; Kinetics and mechanism

1. Introduction

The photochemical activity of platinum complexes has long been known [1]. The primary processes and the origin of intermediates are, however, still poorly understood [1,2]. In many cases, this is due to the fact that for platinum, the two valence forms with stable coordination spheres (Pt(IV) and Pt(II)) are separated by an unstable Pt(III) state. The Pt(III) ion has an electron configuration $5d^7$ whose main therm is degenerate for octahedral complexes [3] and manifestation of the Jan–Teller effect gives a labile coordination sphere. This is related to an existence of numerous short-lived forms of Pt(III) in the photochemistry of many complexes of the Pt(IV) ion [4–6]. The origin of these intermediates can be determined only by fast pulse methods. Thus, for instance, the laser flash photolysis allows one to demonstrate that the photoreduction of $PtCl_6{}^{2-}$ complex in alcohol solutions yields, in succession, five intermediate Pt(III) complexes [7–9]. This, on the one hand, hampers the determination of the mechanism of phototransformations and, on the other hand, can be used in fast and efficient synthesis of new coordination compounds of Pt(II) with amino acids [10,11] and other bioorganic ligands [12,13]. The lability of coordination sphere permits fast introduction of ligands into the environment of Pt(III) ion. These methods of photochemical synthesis are of interest, because some Pt(II) complexes are known to have anti-tumor activity [14].

Scanty information on primary photoprocesses is also typical of nitrite or mixed nitrito-chloride Pt(IV) complexes with high photochemical activity in water solutions [15,16]. Few investigations of the photochemistry of these compounds have been performed either by stationary methods or with insufficient time resolution. The mechanism of primary processes, in this case, was actually unknown. The photochemistry of $Pt(NO_2)_{6-x}Cl_x{}^{2-}$ complexes in water solutions, frozen matrices, and polyvinyl alcohol films has been studied in [16]. All complexes of

---

* Corresponding author. Tel.: +7-3832-332385; fax: +7-3832-342350.
E-mail address: plyusnin@ns.kinetics.nsc.ru (V.F. Plyusnin).

1010-6030/01/$ – see front matter

PII: S1010-6030(01)00463-4

this type display an absorption band with a maximum in the range of 270–280 nm and absorption coefficient of about 25 000–30 000 $M^{-1}\,cm^{-1}$. Light absorption in the range of this band leads to a photoreduction of platinum to the bivalent state with a quantum yield of about 0.5 [16]. The authors assume that for the $Pt(NO_2)_6{}^{2-}$ complex, the primary photoprocess gives the $[Pt(NO_2)_5, NO_2{}^{\bullet}]^{2-}$ pair which either recombines into initial complex or transforms into nitrito-isomer, $[Pt(NO_2)_5(ONO)]^{2-}$, of tetravalent platinum with the optical absorption band at 460 nm. It is suggested that the nitrito-isomer with a rate constant of 80 s^{-1} disappears in the following reaction:

$$[Pt(NO_2)_5ONO]^{2-} \rightarrow [Pt(NO_2)_4]^{2-} + 2NO_2{}^{\bullet} \qquad (1)$$

It is considered that for the $Pt(NO_2)_{6-x}Cl_x{}^{2-}$ nitrito-chloride complexes, the photolysis follows a similar mechanism. The photochemistry of nitrite complexes has been studied in [16] by lamp flash photolysis with a time resolution of about 50 μs which does not allow the record of primary processes. The authors [16] consider that the position of nitrito-isomer absorption band maximum in frozen matrix and liquid solution is quite different ($\lambda_{max} = 330$ and 460 nm, respectively). In addition, a simultaneous formation of two $NO_2{}^{\bullet}$ radicals in reaction (1) is hardly probable. The intermediate states are likely to be involved in these processes.

The goal of the present paper is to study the mechanism of photochemical transformations of *fac*-$Pt(NO_2)_3Cl_3{}^{2+}$ complex by means of laser flash photolysis in nano- and microsecond time domains in wide temperature range in order to record primary intermediates and determine primary photoprocesses.

2. Experimental

The *fac*-$Pt(NO_2)_3Cl_3{}^{2-}$ complex was synthesized as described in [17,18]. The analysis of recrystallized preparation shows the following parameters (found percentage/calculated percentage): Pt + KCl: 66.6/66.49; Pt: 37.8/37.68. The optical spectrum of the substance in water quantitatively coincides with the previous one (strong absorption band with a maximum at 36 230 cm^{-1} (276 nm) and an absorption coefficient of 27 690 $M^{-1}\,cm^{-1}$ [17]). The NMR spectra of ^{195}Pt and ^{14}N were taken at room temperature using a CXP-300 Bruker spectrometer at frequencies of 64.5 and 21.6 MHz. Chemical shifts on scale δ (positive along weak field) were counted relative to the external standards of $NaNO_3$ and H_2PtCl_6. For the latter standard, the shift with respect to a frequency of 21.4 MHz was 4522 ppm. The lines in the NMR spectra of ^{195}Pt were identified according to [19–22]. Deviations of the observed chemical shifts from the published data did not exceed ±10 ppm. When taking into account the great influence of platinum concentration and temperature [23,24] as well as the composition and concentration of salt background [19,20] on the chemical shifts of ^{195}Pt, agreement with the published data is admissible. The chemical shifts in nitrogen NMR spectra have been identified according to [20,23–25].

Solutions were prepared with the help of twice-distilled water. The optical absorption spectra were recorded on Shimadzu UV-2501 and Specord UV–VIS (Carl Zeiss) spectrophotometers. The ESR spectra were taken on “Bruker ESR-300” and “Bruker EMX” spectrometers and 20–50 accumulations were made in each measurement. The spectrum of nonirradiated sample was deducted from all spectra. Radical concentration was calculated using $CuCl_2{\cdot}2H_2O$ microcrystals with the known weight as a central standard. The optical and ESR spectra of low-temperature matrices were recorded using the same sample. To this end, the 7 M LiCl or 4 M $Mg(ClO_4)_2$ water solutions containing the *fac*-$Pt(NO_2)_3Cl_3{}^{2-}$ complex were frozen in a parallel quartz cuvette with a thickness of 0.025 cm and area of 1.6 cm × 0.45 cm in the form of transparent glass. Irradiation was performed by the pulses of XeCl excimer laser (308 nm); for details see [26].

To record the NMR spectra of ^{195}Pt and ^{14}N, solutions were irradiated by a high-pressure DRSh-500 mercury lamp through a set of glassy filters transmitting light with $\lambda >$ 330 nm. Since the concentration of complex in NMR studies exceeded 0.15 M, the degree of phototransformation was controlled by recording the optical spectra of a small amount of irradiated solution in superthin optical quartz cuvettes with a thickness of 10–20 μm.

The laser flash photolysis of solutions and frozen matrices was carried out on a set-up with XeCl excimer laser (308 nm, 15 ns, 50 mJ, beam area on a sample being 10 mm^2) given in detail in [12]. The excited and probing light beams entered the cuvette (thickness being 10 mm) at a small angle of 2°. In experiments at low temperature, the cuvette was placed in a quartz optical cryostat blown out by a stream of cold air with automatically controlled temperature (accuracy of ±0.5°) After each laser pulse, solution was stirred up by a magnetic stirrer. In the flash photolysis of frozen matrices (77 K), the cuvette of 3 mm thickness was located in liquid nitrogen in cryostat. However, to exclude boiling, the laser and probing light beams passed through the cuvette 5 mm higher than the level of liquid nitrogen. After each measurement, the cuvette was unfrozen, the solution was stirred up and frozen again for a new measurement. In some experiments, we used a similar set-up for laser flash photolysis [27] with perpendicular location of exciting and probing light beams. The photomultiplier signal was recorded on a digital Tektronix 7912AD oscillograph connected with an IBM computer. The intensity of laser pulses was measured by the value of optical density of triplet–triplet anthracene absorption in the oxygen-free benzene solution at 431 nm (quantum yield of the triplet state is 0.53 and absorption coefficient is 42 000 $M^{-1}\,cm^{-1}$ [28]).

In numerical calculations of the kinetics of the disappearance of an intermediate optical absorption, the differential equations were solved by the fourth-order Runge–Cutta method and special program. The ESR spectra of radical particles resulting from photolysis of frozen matrices were modeled using a special program with respect to the anisotropy of hyperfine structure, g-factor, and linewidths. To determine absorption coefficients of intermediate absorption arising in experiments on laser flash photolysis, solution was irradiated in quartz microcuvettes of 50 μl volume (2 mm × 5 mm × 5 mm) with an optical thickness of 5 mm. After one laser pulse, the intermediate absorption was recorded on a set-up for flash photolysis. Thereafter, spectrophotometer was used to determine a decrease in the optical density of the band with a maximum of 36 230 cm^{-1} (276 nm) of the initial *fac*-$Pt(NO_2)_3Cl_3^{2-}$ complex by a change of the optical spectrum. The known absorption coefficient of this band ($\varepsilon = 27\,690\,M^{-1}\,cm^{-1}$) was used to determine the absorption coefficient of intermediate absorption.

3. Results and discussion

3.1. Stationary photolysis of *fac*-$Pt(NO_2)_3Cl_3^{2-}$ solutions

The optical spectra of the solutions of the octahedral complexes of Pt(IV) ion with nitrite groups ranging from six to four in the coordination sphere (the rest of the particles being Cl^- ions) have two strong absorption bands with the maxima at 280 and 330 nm (35 700 and 30 300 cm^{-1}) and absorption coefficients $(2.15\text{–}3.4) \times 10^4$ and $(7.5\text{–}12.1) \times 10^3\,M^{-1}\,cm^{-1}$, respectively [16]. These bands refer to transitions with electron transfer from ligands to metal (LMCT transitions) involving both nitrite and chloride ions, because the $PtCl_6^{2-}$ complex also has absorption bands at 265 and 360 nm (37 700 and 27 800 cm^{-1}) with absorption coefficients of 2.8×10^4 and 500 $M^{-1}\,cm^{-1}$ [29]. Decomposing the optical spectrum of the water solution of *fac*-$Pt(NO_2)_3Cl_3^{2-}$ complex (three nitrite groups) into Gaussian components shows that it has absorption bands with maxima at 207, 276, and 320 nm (48 400, 36 230, and 31 300 cm^{-1}). The intraligand transition for the nitrite Pt(IV) complexes can contribute to absorption only in the region of 210 nm (47 700 cm^{-1}) where the free NO_2^- ion in water solutions has absorption band with an absorption coefficient of $0.54 \times 10^4\,M^{-1}\,cm^{-1}$ [30]. In more long-wave region, the NO_2^- ion displays weaker absorption bands at 355 and 287 nm (28 200 and 34 800 cm^{-1}) with absorption coefficients of 22.5 and 9.4 $M^{-1}\,cm^{-1}$ [30].

A change in the optical spectrum of the water solution of *fac*-$Pt(NO_2)_3Cl_3^{2-}$ complex under irradiation of the XeCl excimer laser (308 nm) includes two stages. Initially, there is an isosbestic point at 230 nm (43 500 cm^{-1}) (Fig. 1) which is then disappearing and a new absorption band is formed with a maximum at 210 nm (47 560 cm^{-1}), typical for Pt(II) complexes. Photoreduction of Pt(IV) to Pt(II) is confirmed by the study of NMR spectra on the ^{195}Pt and ^{14}N nuclei. Fig. 2 shows the NMR spectrum (^{195}Pt) of the irradiated solution. The remaining signal of the initial *fac*-$Pt(NO_2)_3Cl_3^{2-}$ complex (1384 ppm) is observed along with that of the tetravalent platinum complex ($Pt(NO_2)_6^{2-}$) (2103 ppm, 14% of the disappearing initial complex) and the signals of the bivalent platinum $Pt(NO_2)Cl_3^{2-}$ (−1648 ppm, 11%) and $Pt(NO_2)_2(H_2O)_2$ (−1774 ppm, 73%).

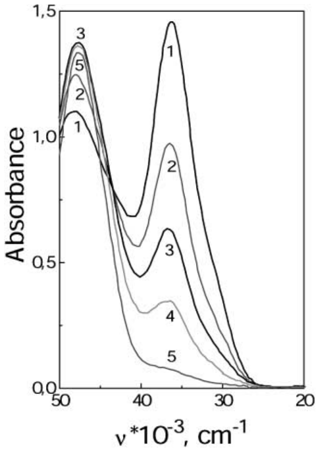

Fig. 1. A change in the optical spectrum of the water solution of *fac*-$Pt(NO_2)_3Cl_3^{2-}$ complex under irradiation by a high-pressure mercury lamp (DRSh-500) through a filter transmitting lines 313, 334, and 365 nm. The initial concentration of the complex is 2.9×10^{-4} M, the cuvette thickness 2 mm, $T = 298$ K. Curves (1)–(5): irradiation during 0, 1, 2, 5, and 20 s, respectively.

The ^{14}N spectrum of this solution shows both the wide signal with a center at +51 ppm corresponding to the NO_2^- group coordinated with platinum ions and the strong narrow line of the free NO_3^- ion. There is also a weak signal of water-dissolved N_2 (−66.7 ppm) and the weak wide unidentified signal with a center at $\delta = +4$ ppm.

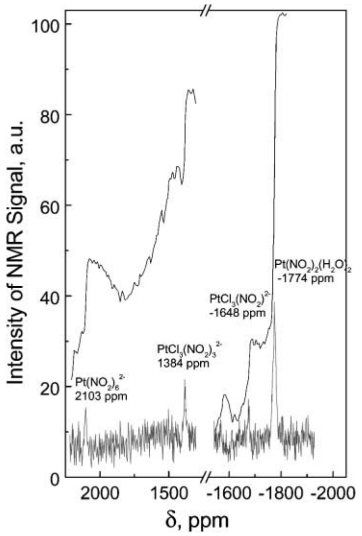

Fig. 2. NMR spectrum on the ^{295}Pt nucleus of the irradiated *fac*-$Pt(NO_2)_3Cl_3^{2-}$ water solution. Initial concentration of the complex is 0.16 M, solution volume 10 ml, irradiation time 40 min through a set of filters transmitting lines 313, 334, and 365 nm of the high-pressure mercury lamp.

It will be shown that the $Pt(NO_2)Cl_3^{2-}$ complex arises from a chain of transformations of the excited initial *fac*-$Pt(NO_2)_3Cl_3^{2-}$ complex. The formation of $Pt(NO_2)_6^{2-}$ and $Pt(NO_2)_2(H_2O)_2$ complexes is, probably, determined by the processes of ligand substitution and secondary photolysis of the $Pt(NO_2)Cl_3^{2-}$ complex. To determine the primary processes, we have studied the changes in the optical and ESR spectra upon photolysis of frozen matrices, and recorded the optical spectra of intermediates resulting from the laser flash photolysis of *fac*-$Pt(NO_2)_3Cl_3^{2-}$ solutions.

3.2. Steady-state photolysis of frozen matrices containing fac-$Pt(NO_2)_3Cl_3^{2-}$ complex

The optical spectrum of the *fac*-$Pt(NO_2)_3Cl_3^{2-}$ complex in a low-temperature matrix (7 M LiCl in water, 77 K) changes little as compared with water solutions of this complex at room temperature. Decomposition into the Gaussian components shows that the spectrum (Fig. 3) contains bands with maxima at 212, 272, and 311 nm (47 250, 36 800, and 32 200 cm^{-1}, respectively).

The optical spectrum of the *fac*-$Pt(NO_2)_3Cl_3^{2-}$ complex vanishes in the low-temperature matrix under either the light of the high-pressure mercury lamp (through the filter passing the lines 313, 334, and 365 nm) or the pulses of XeCl excimer laser (308 nm) with the preservation of two isosbestic points at 254 and 336 nm (39 360 and 29 740 cm^{-1}) and the appearance of new absorption bands. Fig. 3 (spectrum (6)) shows the calculated final spectrum that would form with the conservation of isosbestic points until the initial complex disappears. It contains bands with maxima at 228 and 334 nm (43 900 and 30 000 cm^{-1}) with absorption coefficients of 2×10^4 and 4.3×10^3 M^{-1} cm^{-1}. The isosbestic points fail under prolonged irradiation and the bands forming in the first stage disappear, i.e. the primary product also manifests its photochemical activity. Similar changes in the optical spectrum are also observed for the *fac*-$Pt(NO_2)_3Cl_3^{2-}$ complex and in the low-temperature 4 M $Mg(ClO_4)_2$ matrix.

To determine the nature of primary processes and the origin of a new optical spectrum of importance is the study of ESR spectra arising from photolysis of low-temperature matrices containing the *fac*-$Pt(NO_2)_3Cl_3^{2-}$ complex. Fig. 4 demonstrates the ESR spectrum of $NO_2^{\bullet}$ radical resulting from prolonged irradiation of such a matrix. Numerical calculations show that parameters of an anisotropic ESR spectrum and values of hyperfine splitting constants correspond to the literature values [31–36] ($g_{xx} = 2.0066$, $g_{yy} = 1.9920$, $g_{zz} = 2.0022$, $A_{xx} = 50.6$ G, $A_{yy} = 49.6$ G, $A_{zz} = 70.2$ G, $A_{\rm iso} = 56.8$ G for $NO_2^{\bullet}$ in the 7 M LiCl matrix which coincides with the parameters for this radical in ice at 77 K [32]). Fig. 4 also shows a change in the intensity of a new optical band with a maximum at 30 000 cm^{-1} (333 nm) and the concentration of the $NO_2^{\bullet}$ radical determined by means of ESR spectroscopy under irradiation. It is noteworthy that the intensity of the optical band reaches its maximum when there is actually no signal of $NO_2^{\bullet}$ radical in the ESR spectrum. Thus, the $NO_2^{\bullet}$ radicals appear

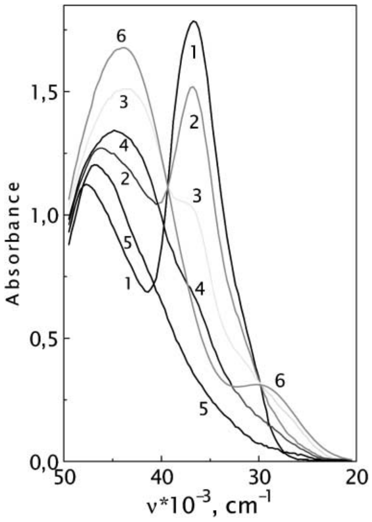

Fig. 3. A change in the optical spectrum of the frozen (77 K) 7 M LiCl solution in H_2O containing 2×10^{-3} M of the *fac*-$Pt(NO_2)_3Cl_3^{2-}$ complex under irradiation by the XeCl excimer laser (308 nm, 10 mJ, 10 Hz). The cuvette thickness is 250 μm. Curves (1)–(5): irradiation during 0.01, 1, 20, and 200 min, respectively; curve (6): the calculated final spectrum with conservation of the isosbestic point at 30 000 cm^{-1} to complete disappearance of the initial complex.

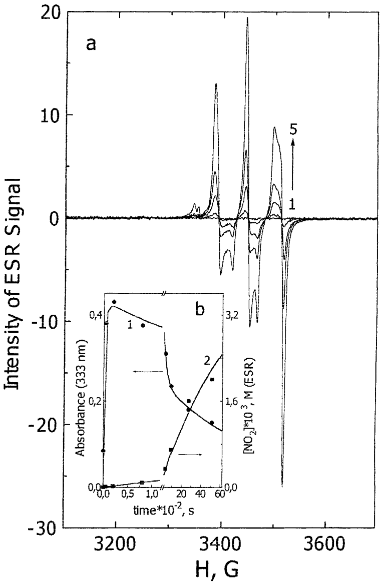

Fig. 4. ESR spectrum of $NO_2^{\bullet}$ radical (a) appearing under irradiation of the frozen (77 K) matrix (7 M LiCl in H_2O) containing 4.3×10^{-3} M of the *fac*-$Pt(NO_2)_3Cl_3^{2-}$ complex. Solution is frozen in a plane-parallel cuvette 250 μm thick and with area $S = 1.6 \times 0.45$ cm^2, for which the optical and ESR spectra were taken. Irradiation was performed by the XeCl excimer laser pulses (308 nm, 10 mJ, 10 Hz). Curves (1)–(5): irradiation during 5, 80, 320, 920, and 5120 s, respectively. Insert (b) shows the kinetics of a change in the intensity of optical band (1) with a maximum at 30 000 cm^{-1} (333 nm) (Fig. 3) and $NO_2^{\bullet}$ concentration calculated by integrating ESR spectra (2).

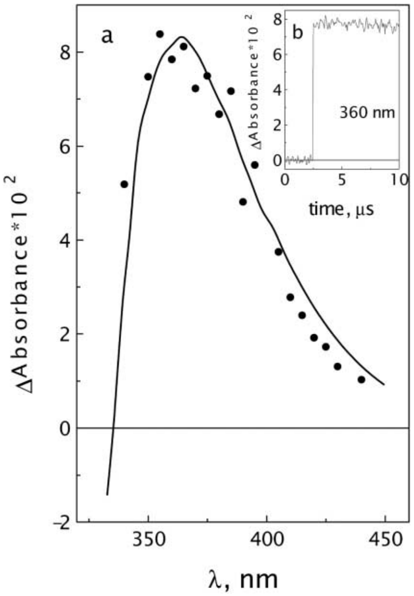

Fig. 5. Laser flash photolysis (a) of the frozen (77 K) matrix (7 M LiCl in H_2O) containing 5×10^{-4} M of the *fac*-$Pt(NO_2)_3Cl_3{}^{2-}$ complex. Cuvette thickness is 3 mm. The dots denote absorption spectrum following the laser pulse. Solid line denotes a change in the stationary spectrum (the difference in spectra (6) and (1) taken from Fig. 3 with normalization to 365 nm). Insert (b) shows a typical kinetic curve.

upon the secondary photolysis of an intermediate particle whose optical spectrum is shown by spectrum (6) in Fig. 3.

It is assumed [16] that this intermediate is a nitrito-isomer of the Pt(IV) complex. In our case, it is $Pt(NO_2)_2(ONO)Cl_3{}^{2-}$ forming upon relaxation of the primary radical pair $[Pt(NO_2)_2Cl_3, NO_2{}^{\bullet}]^{2-}$. Note that the photochemical transformation of the nitrito-isomers from the initial nitro-form has been first revealed for a $Co(NH_3)_5(NO_2)^{2+}$ complex [37]. This reaction occurs not only in solutions, but also in crystals [38], which allows one to assume the intramolecular character of nitrito-isomer formation. No evidence is available for the kinetics of this transformation. However, according to laser flash photolysis, for the *fac*-$Pt(NO_2)_3Cl_3{}^{2+}$ complex, the new optical spectrum appears during the time shorter than 50 ns (Fig. 5) even in the frozen matrix (77 K).

The secondary photolysis of nitrito-isomers leads to the appearance of the pair particles — the $NO_2{}^{\bullet}$ radical and the paramagnetic Pt(III) ion as the $Pt(NO_2)_2Cl_3{}^{2-}$ complex (electron configuration $5d^7$, spin 1/2). When the distance between partners is 5 A, the dipole linewidth ($\Delta H \sim 2g_e\beta/r^3$) can reach 300 G. The fast spin-lattice relaxation (T_1) of the ion can decrease the dipole broadening ($\Delta H \sim (2g_e\beta/r^3)^2 T_1$). However, even at very short times, $T_1 \sim 10^{-10}$ s, typical of the paramagnetic ions of transient metals [39], the linewidth decreases only to 30 G. In experimental spectra at amplitudes exceeding the level of noise, the linewidth determined from the extreme high-field component (Fig. 4) is substantially less than the above estimates and decreases from 12.6 to 5.7 G with prolonged irradiation and an increase in $NO_2{}^{\bullet}$ concentration. Thus, the radical–ion distance can exceed 5 A already during the photochemical dissociation of the nitrito-isomer and increase upon the photolysis, thus reaching 15–20 A. Below, using the laser flash photolysis, we show that in liquid solution, the nitrito-isomer thermally dissociates with an activation energy of about 0.5 eV (48.6 kJ mol^{-1}). The great excess energy forming with the energy of absorbed quantum amounting to about 4 eV (308 nm) is transferred to the translational degree of radical freedom and can give substantial radical–ion distances. A decrease in the linewidth under prolonged photolysis can be caused by the absorption of laser light quanta (308 nm) by the $NO_2{}^{\bullet}$ radical (the optical spectrum of the radical represents a wide band with a maximum at 400 nm and absorption coefficient of 200 M^{-1} cm^{-1} [40]). Relaxation of radical excitation electron energy into the thermal one causes the local heating of matrix, the appearance of radical mobility, an increase in radical–ion distance, a decrease in the dipole–dipole interaction of partners in a pair, and a decrease in linewidths in the radical ESR spectrum.

Note that an alternative process accounting for the behavior of optical and ESR spectra under irradiation can be a formation of a divided $\{[Pt(NO_2)_2Cl_3]^{2-}\ldots NO_2{}^{\bullet}\}$ pair from the primary radical $[Pt(NO_2)_2Cl_3, NO_2{}^{\bullet}]^{2-}$ pair. In this case, the band with a maximum at 30 000 cm^{-1} will belong to the $[Pt(NO_2)_2Cl_3]^{2-}$ complex. The absence of the ESR spectrum of $NO_2{}^{\bullet}$ radical at the instant the absorption maximum is reached at 30 000 cm^{-1} can be assigned, in this case, to the above strong dipole–dipole paramagnetic radical–ion interaction. The appearance of $NO_2{}^{\bullet}$ lines under prolonged irradiation of the sample can be also attributed to the optical absorption of this radical. However, the kinetic studies by laser flash photolysis show that the primary process is the nitrito-isomer formation.

3.3. *Laser flash photolysis of fac-$Pt(NO_2)_3Cl_3{}^{2-}$ solutions*

Fig. 6 shows the optical spectra and the kinetic curves of intermediate absorption for the *fac*-$Pt(NO_2)_3Cl_3{}^{2-}$ complex in the cold water 7 M LiCl solution at 252 K (these solutions remain in liquid state down to about 170 K). A laser pulse causes an appearance of an absorption with an effective maximum at 360 nm. At 10 μs, the maximum shifts to 375 nm and a bleaching appears (negative values of changes in the optical density) at $\lambda < 350$ nm. The same figure shows that the spectrum of bleaching at long times is determined by the disappearance of initial complex absorption. This spectrum is found by stationary spectrophotometric measurements of the initial solution and after irradiation. The insert in Fig. 6c shows that real optical spectra of the intermediate particles arise after the laser pulse (50 ns) and 10 μs. These were obtained by deducing the stationary spectrum of bleaching from the absorption spectra at these times. Absorption identical to that (the band near 30 000 cm^{-1}) in the frozen matrix under stationary photolysis is observed in a cold liquid solution. However, at 10 μs this absorption disappears

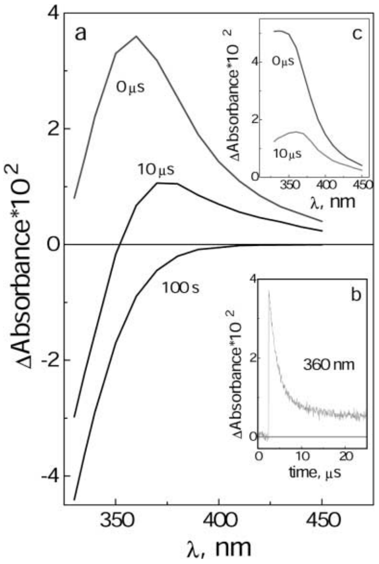

Fig. 6. Intermediate optical spectra (a) appearing from laser flash photolysis of the cold (252 K) 7 M LiCl solution in H_2O containing the *fac*-$Pt(NO_2)_3Cl_3{}^{2-}$ complex (7.3×10^{-5} M). Cuvette thickness is 1 cm. Curves (1)–(3): the spectra just after the pulse, after 10 μs and the spectrum of bleaching owing to the disappearance of the part of initial complex (8.4×10^{-6} M) measured on a spectrophotometer after one laser pulse. Insert (b) shows a typical kinetic curve. Insert (c) shows the real optical spectra of intermediates arising just after the pulse and after 10 μs. These are obtained by deducting the stationary bleaching spectrum (3) from spectra (1) and (2).

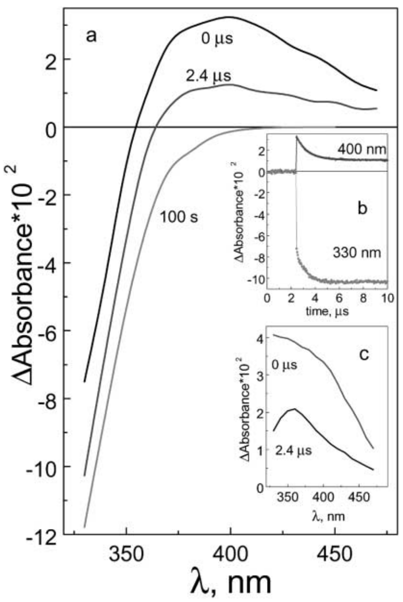

Fig. 7. Intermediate optical spectra (a) arising from laser flash photolysis of the cold (274 K) water solution of the *fac*-$Pt(NO_2)_3Cl_3{}^{2-}$ complex (concentration is 1×10^{-4} M, cuvette thickness is 1 cm). Curves (1)–(3): the spectra just after the pulse, after 2.4 μs and the bleaching spectrum owing to the disappearance of the part of initial complex (1.8×10^{-5} M) measured on a spectrophotometer after one laser pulse. Insert (b) shows typical kinetic curves. Insert (c) shows the optical spectra of intermediates arising just after the pulse and after 2.4 μs. These are obtained by deducting stationary bleaching spectrum (3) from spectra (1) and (2).

and a more long-lived absorption remains in the spectrum as a band with a maximum in the region of 360 nm.

A decrease in the initial *fac*-$Pt(NO_2)_3Cl_3{}^{2-}$ complex concentration determined by stationary measurements in a microcuvette after a single laser pulse allows one to estimate the absorption coefficients of both intermediate absorption bands. For the former band with a maximum at 30 000 cm^{-1} (333 nm), the absorption coefficient is 4700 ± 500 M^{-1} cm^{-1} which actually coincides with the value for the frozen matrix (4300 M^{-1} cm^{-1}). The latter absorption band with a maximum at 360 nm remaining in the spectrum by 10 μs has the absorption coefficient of 900 ± 200 M^{-1} cm^{-1}.

In a cold (274 K) water solution of the *fac*-$Pt(NO_2)_3Cl_3{}^{2-}$ complex, the laser pulse causes changes in optical density that are similar to those in 7 M LiCl solutions. Fig. 7 shows the kinetics of the intermediate optical absorption and the spectra of the solution after the laser pulse (50 ns) in 2.4 μs and the stationary spectrum of bleaching at long times measured upon photolysis in a microcuvette. The insert shows absorption spectra arising just after the pulse and at time 2.4 μs. After the pulse, the band appears with a maximum near 30 000 cm^{-1} (333 nm), which rapidly vanishes and 2.4 μs later is substituted by a more long-lived band with a maximum at 360 nm. The absorption coefficients of these bands estimated in pulse and stationary measurements in a microcuvette are 1700 ± 300 and 900 ± 200 M^{-1} cm^{-1}, respectively. In this case, the primary band is broader (Fig. 7c) and its absorption coefficient is smaller than that of 7 M LiCl solutions. Some changes in its form can be caused by the dependence of spectrum on solvent.

According to the optical and ESR data on the photolysis of frozen matrices, the band with a maximum near 30 000 cm^{-1} in both water and LiCl solutions can be assigned to the appearance of the $Pt(NO_2)_2(ONO)Cl_3{}^{2-}$ nitrito-isomer. The fast kinetics of this absorption disappearance is due to the thermal dissociation of the complex

$$Pt(NO_2)_2(ONO)Cl_3{}^{2-} \rightarrow Pt(NO_2)_2Cl_3{}^{2-} + NO_2{}^{\bullet} \qquad (2)$$

In a solid frozen matrix, the thermal dissociation is impossible. Photodissociation, however, leads to an appearance of the ESR spectrum of $NO_2{}^{\bullet}$ radical. The more long-lived absorption in the form of a band with a maximum at 360 nm observed in the spectrum at 2.4 μs (H_2O) and 10 μs (7 M LiCl) belongs, in this case, to the sum of the spectra of trivalent platinum $Pt(NO_2)_2Cl_3{}^{2-}$ and $NO_2{}^{\bullet}$ radical. Since the end products of photolysis are the Pt(II) complexes, the $Pt(NO_2)_2Cl_3{}^{2-}$ complex is assumed to dissociate as well,

$$Pt(NO_2)_2Cl_3{}^{2-} \rightarrow Pt(NO_2)Cl_3{}^{2-} + NO_2{}^{\bullet} \qquad (3)$$

Dissociation caused by chlorine atom appearance can be excluded, because in 7 M LiCl solutions this atom must rapidly convert into a $Cl_2{}^{\bullet -}$ radical ion, which has a strong absorption band with a maximum at 340 nm ($\varepsilon = 12\,000$

$M^{-1}\,cm^{-1}$ [41]). This band, however, is not recorded in pulse experiments. The kinetics of dissociation reaction (3) is manifested in a decrease in the absorption band intensity at 360 nm after the fast disappearance of nitrito-isomer. It is complicated by the fact that the $NO_2^{\bullet}$ radical has a fairly wide band of optical absorption with a maximum at 400 nm ($\varepsilon = 200\,M^{-1}\,cm^{-1}$ [40]), and can rapidly and reversibly recombine [40,42,43],

$$NO_2^{\bullet} + NO_2^{\bullet} \rightleftarrows N_2O_4 \qquad (4)$$

The equilibrium constant for $NO_2^{\bullet}$ radicals dimerization is known for water solutions at room temperature ($1.5 \times 10^{-5}\,M^{-1}$ [40,42,43]). The rate constant of the direct reaction in these conditions is $9.0 \times 10^{8}\,M^{-1}\,s^{-1}$ and that of the reverse reaction is $1.17 \times 10^{4}\,s^{-1}$ [42]. The N_2O_4 molecule has the absorption band with a maximum at 335 nm ($\varepsilon = 320\,M^{-1}\,cm^{-1}$ [40]), and in addition to the reaction of reverse dissociation into two radicals, it can disappear in the reaction with water,

$$N_2O_4 + H_2O \rightarrow NO_2^{-} + NO_3^{-} + 2H^{+} \qquad (5)$$

with a rate constant of $1.0 \times 10^{3}\,s^{-1}$ [40,42]. At 400 nm, the initial *fac*-$Pt(NO_2)_3Cl_3^{2-}$ complex and N_2O_4 dimer do not actually absorb. At this wavelength, it is convenient to model experimental kinetics for determination of the reaction rate constants.

Fig. 8a–c shows the experimental kinetic curve of the disappearance of the intermediate absorption at 400 nm for the *fac*-$Pt(NO_2)_3Cl_3^{2-}$ water solution at room temperature in different time domains. Fig. 8 also shows the calculated curves of the decrease in the optical density. The calculations involve the literature data on the rate constants of reactions (4) and (5) and the absorption coefficients of the absorption band of the $NO_2^{\bullet}$ radical. The absorption coefficient at the maximum of $Pt(NO_2)_2(ONO)Cl_3^{2-}$ absorption band ($30\,000\,cm^{-1}$) is given above and it is $1400\,M^{-1}\,cm^{-1}$ at 400 nm. The rate constants of reactions (2) and (3) and the absorption coefficients of the $Pt(NO_2)_2Cl_3^{2-}$ complex were varied. The calculated results indicate that in the framework of the scheme of reactions (2)–(5), the kinetics at short times is well described (Fig. 8a and b, curve 2). The rate constants of the dissociation of the nitrito-isomer (2) and the $Pt(NO_2)_2Cl_3^{2-}$ complex (3) are 3.2×10^{6} and $1.5 \times 10^{5}\,s^{-1}$, respectively, which correspond to the life times of 0.3 and 7 μs of these particles. The absorption coefficient of $Pt(NO_2)_2Cl_3^{2-}$ at 400 nm is $360\,M^{-1}\,cm^{-1}$ (at the maximum of the absorption band of this particle at 360 nm, $\varepsilon = 720\,M^{-1}\,cm^{-1}$) with respect to the contribution of the $NO_2^{\bullet}$ absorption.

At longer times (>10 μs), the calculated kinetics lie substantially lower than the experimental ones (Fig. 8a, curve 1). Thus, the optical absorption decreases slower than it follows from the literature values of constants. Varying constants gives no agreement between the calculated and experimental curves, because at initial concentrations of the $NO_2^{\bullet}$ radical in the range of $(1–10) \times 10^{-5}$ M, it is substantially (by 50–80%) dimerized and the N_2O_4 dimer does not absorb at 400 nm. We assume that the effect of long kinetic curves can be related to the reversible reaction of $Pt(NO_2)_2Cl_3^{2-}$ complex dissociation, i.e. to the existence of the reverse reaction of $NO_2^{\bullet}$ radical coordination which substantially increases the life time of this complex,

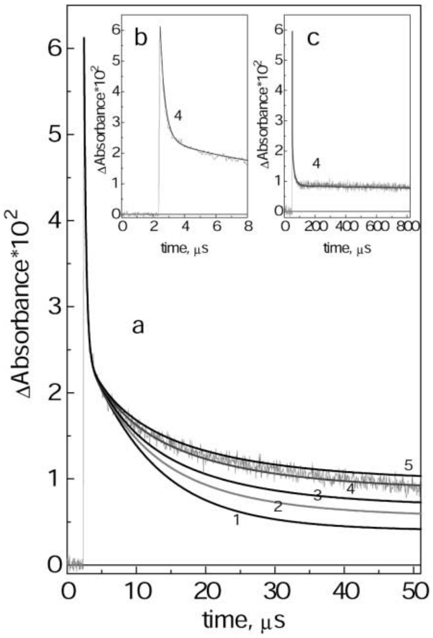

Fig. 8. Experimental kinetic curve of the disappearance of intermediate optical absorption after laser pulse for water *fac*-$Pt(NO_2)_3Cl_3^{2-}$ solution (1×10^{-4} M, cuvette thickness is 1 cm) at room temperature at different time sweeps (a, b, c). Solid lines denote numerical calculation of kinetics by the scheme of reactions (2)–(6) with rate constants $k_2 = 3.2 \times 10^{6}\,s^{-1}$, $k_3 = 1.5 \times 10^{5}\,s^{-1}$, $k_4 = 9.0 \times 10^{8}\,M^{-1}\,s^{-1}$, $k_{-4} = 1.17 \times 10^{4}\,s^{-1}$, $k_5 = 1 \times 10^{3}\,s^{-1}$. For curves (1)–(5), $k_6 = 0$, 1×10^{9}, 2×10^{9}, 4.2×10^{9}, $6 \times 10^{9}\,s^{-1}$, respectively.

$$Pt(NO_2)Cl_3^{2-} + NO_2^{\bullet} \rightarrow Pt(NO_2)_2Cl_3^{2-} \qquad (6)$$

Taking into account this reaction and the value $k_6 = 4.2 \times 10^{9}\,M^{-1}\,s^{-1}$, we attain a fair agreement between calculated and experimental kinetics (Fig. 8a, curve 4). Thus, we get the equilibrium constant for the reversible dissociation of $Pt(NO_2)Cl_3^{2-}$, $K = k_3/k_6 = 3.6 \times 10^{-5}$ M. Note that the reverse coordination of $NO_2^{\bullet}$ is quite common for the photochemistry of coordination compounds. Thus, for example under laser flash photolysis of the Mn(III)TPP(ONO) complex in various solvents, it has been established that the $NO_2^{\bullet}$ radical arising after the light pulse inversely coordinates with the Mn(II)TPP complex at a high rate constant of $2.2 \times 10^{9}\,M^{-1}\,s^{-1}$ in benzene [44].

The existence of reaction (6) leads to a noticeable increase in the effective life time of the $Pt(NO_2)_2Cl_3^{2-}$ complex which can reach the millisecond range (Fig. 8c). Probably, this process rather than the long-lived nitrito-isomer accounts for absorption with a characteristic time of

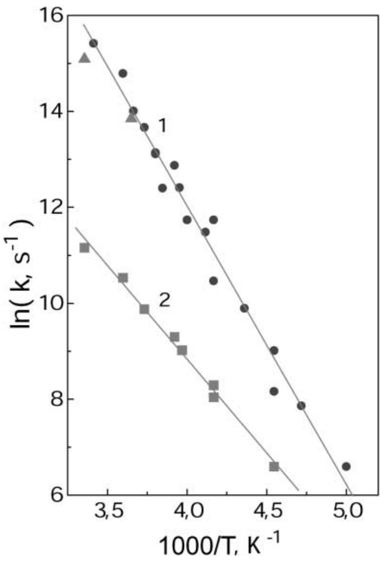

Fig. 9. Dependence of the rate constants of the dissociation of nitrito-isomer $Pt(NO_2)_2(ONO)Cl_3{}^{2-}$ (1) and $Pt(NO_2)_2Cl_3{}^{2-}$ complex (2) on inverse temperature. Two triangles in (1) are for water solution and circles are for 7 M LiCl solutions.

disappearance of about 10 ms observed [16] in experiments on lamp flash photolysis. Actually, a decrease in the concentration of the $Pt(NO_2)_2Cl_3{}^{2-}$ complex in these conditions is determined by the reaction of N_2O_4 dimer with water (reaction (5)).

A drop in solution temperature causes substantial increase in the typical times of dissociation of the intermediate platinum complexes. We have already presented the data on flash photolysis of cold water–salt (7 M LiCl) solutions of *fac*-$Pt(NO_2)_3Cl_3{}^{2-}$ at 252 K (Fig. 6). Similar kinetic curves for these solutions have been obtained within a wide temperature range of 200–300 K. There are no data on the dependence of the rate constants of reactions (4) and (5) on the temperature and concentration of LiCl necessary for the complete calculation of kinetics in these conditions. However, the numerical calculations of kinetics and comparison with the experimental ones obtained for pure water solutions at room temperature show that the satisfactory values of k_2 and k_3 can be derived by treating the initial part of experimental curves with respect to two exponents. The k_2 value is obtained, in this case, to within high accuracy, owing to the relation $k_2 \gg k_3$. Fig. 9 shows the dependences of rate constants k_2 and k_3 of the dissociation of complexes $Pt(NO_2)_2(ONO)Cl_3{}^{2-}$ and $[Pt(NO_2)_2Cl_3]^{2-}$ obtained by the two-exponential treatment of the initial parts of kinetic curves on the reverse temperature for 7 M LiCl solutions. The activation energies of these processes are 48.6 ± 1.7 and $37.6 \pm 1.5\,\mathrm{kJ\,mol^{-1}}$, respectively. Two points for pure water solutions at 298 and 274 K are in fair agreement with the data on 7 M LiCl solutions.

We have already mentioned the possibility of an alternative process of the formation of the divided pair $\{[Pt(NO_2)_2Cl_3]^{2-} \ldots NO_2{}^{\bullet}\}$ in the primary photochemical process. In this case, at room temperature in water solution, the band with a maximum at $30\,000\,\mathrm{cm^{-1}}$ and life time of about 300 ns must belong to the $[Pt(NO_2)_2Cl_3]^{2-}$ complex. The dissociation of this particle (reaction (3)) results in the formation of the complex of bivalent platinum ion, which usually has a more stable coordination sphere and absorption in the far UV spectrum region. Therefore, in this alternative process, the origin of the second band ($\lambda_{max} = 360$ nm) with a fairly high absorption coefficient ($\varepsilon = 720\,\mathrm{M^{-1}\,cm^{-1}}$) that disappears with a typical time of 7 μs is unclear. The appearance of $NO_2{}^{\bullet}$ radical and the kinetics of its disappearance cannot be explained by the existence of the second band, because the radical has the band with a maximum at 400 nm and the absorption coefficient that is several times smaller ($\varepsilon = 200\,\mathrm{M^{-1}\,cm^{-1}}$).

4. Conclusions

The data on laser flash photolysis of solutions and photolysis of frozen matrices involving optical spectroscopy and ESR methods show that excitation at 308 nm causes photoisomerization of *fac*-$Pt(NO_2)_3Cl_3{}^{2-}$ complex, resulting in the formation of the $Pt(NO_2)_2(ONO)Cl_3{}^{2-}$ nitrito-form. Under prolonged irradiation, the light starts to absorb the nitrito-isomer, subject to the reaction of photodissociation giving the lines of free $NO_2{}^{\bullet}$ radical in the ESR spectrum in frozen matrices. Without irradiation, the nitrito-isomer is stable in a frozen matrix. In liquid solution, however, it rapidly dissociates into $[Pt(NO_2)_2Cl_3]^{2-}$ and $NO_2{}^{\bullet}$ radical. The intermediate complex of trivalent platinum $[Pt(NO_2)_2Cl_3]^{2-}$ also dissociates into bivalent platinum and the second $NO_2{}^{\bullet}$ radical. The characteristic times of these processes are 300 ns and 7 μs, respectively. According to the data of NMR spectroscopy, the complexes of bivalent platinum are subject to further dark and photochemical reactions of ligand substitution.

Acknowledgements

The financial support of the Russian Foundation for Basic Research (Grant nos. 99-03-33308 and 99-03-32272) and Russian Federal Scientific Program "Integration" (Grant no. 274) is gratefully acknowledged. Authors also would like to thank Dr. A.A. Shubin for the program of computer simulation of ESR spectra.

References

[1] V. Balzani, V. Carrassity, Photochemistry of Coordination Compounds, Academic Press, London, 1970.
[2] J. Sykora, J. Sima, Coord. Chem. Rev. 107 (1990) 1.
[3] A. Goursot, H. Chermette, E. Penigault, M. Chanon, W.L. Waltz, Inorg. Chem. 23 (1984) 3618.

[4] R.L. Rich, H. Taube, J. Am. Chem. Soc. 76 (1954) 2608.

[5] K.P. Balashev, I.I. Blinov, G.A. Shagisultanova, J. Inorg. Chem. (Russ.) 32 (1987) 2470.

[6] A. Goursot, A.D. Kirk, W.L. Walz, G.B. Porter, D.K. Sharma, Inorg. Chem. 26 (1987) 14.

[7] V.P. Grivin, I.V. Khmelinski, V.F. Plyusnin, J. Photochem. Photobiol. A: Chem. 51 (1990) 379.

[8] V.P. Grivin, I.V. Khmelinski, V.F. Plyusnin, I.I. Blinov, K.P. Balashev, J. Photochem. Photobiol. A: Chem. 51 (1990) 167.

[9] V.P. Grivin, I.V. Khmelinski, V.F. Plyusnin, J. Photochem. Photobiol. A: Chem. 59 (1991) 153.

[10] V.P. Grivin, V.F. Plyusnin, I.V. Khmelinski, M. Mitewa, P.R. Bontchev, J. Photochem. Photobiol. A: Chem. 62 (1991) 15.

[11] V.F. Plyusnin, V.P. Grivin, L.F. Krylova, L.D. Dikanskaja, Yu.V. Ivanov, H. Lemmetyinen, J. Photochem. Photobiol. A: Chem. 104 (1997) 45.

[12] V.P. Grivin, V.F. Plyusnin, I.V. Khmelinski, N.M. Bazhin, M. Mitewa, P.R. Bontchev, J. Photochem. Photobiol. A: Chem. 51 (1990) 371.

[13] V.P. Grivin, V.F. Plyusnin, I.V. Khmelinski, M. Mitewa, J. Angelova, E. Dimitrova, P.R. Bontchev, J. Photochem. Photobiol. A: Chem. 63 (1992) 7.

[14] B. Rosenberg, Platin. Met. Rev. 15 (1971) 42.

[15] V. Balzani, N. Sabbatiny, V. Carrassity, Progress in Coordination Chemistry, North-Holland, Amsterdam, 1968.

[16] K.P. Balashev, I.I. Blinov, G.A. Shagisultanova, Coord. Chem. (Russ.) 11 (1985) 1121.

[17] A.V. Babaeva, N.I. Ushakova, Proceed. Inst. Platin. (Russ.) N27 (1952) 164.

[18] I.I. Chernjaev, L.Yu. Genning, Proceed. Inst. Platin. (Russ.) N11 (1933) 45.

[19] S.J.S. Kerrison, P. Sadler, J. Chem. Soc., Dalton Trans. (1982) 2363.

[20] M.A. Fedotov, S.V. Korenev, A.V. Beljaev, Coord. Chem. (Russ.) 16 (1990) 1272.

[21] F.E. Wood, A.L. Balch, Inorg. Chim. Acta 76 (1983) L63.

[22] T.G. Appleton, J.R. Hall, S.F. Ralph, Inorg. Chem. 24 (1985) 4685.

[23] B.E. Mann, R.K. Harris (Eds.), NMR and Periodic Table, Academic Press, London, 1978.

[24] I.J. Mason, Multinuclear NMR, Plenum Press, New York, 1987.

[25] S.P. Gabuda, R.N. Pletnev, M.A. Fedotov, Nuclear Magnetic Resonance in Inorganic Chemistry, Nauka, Moscow, 1988.

[26] V.V. Korolev, V.F. Plyusnin, N.M. Bazhin, J. Phys. Chem. (Russ.) 49 (1975) 2440.

[27] H. Lemmetyinen, R. Ovaskainen, K. Nieminen, K. Vaskonen, I. Sychtchikova, J. Chem. Soc., Perkin Trans. (1992) 113.

[28] R.H. Compton, T.V. Grattan, T. Morrow, J. Photochem. 14 (1980) 61.

[29] D.L. Swihart, W.R. Mason, Inorg. Chem. 9 (1970) 1749.

[30] M. Fischer, P. Warnek, J. Phys. Chem. 100 (1996) 18749.

[31] H. Zeldes, R. Livingston, J. Chem. Phys. 35 (1961) 563.

[32] P.W. Atkins, N. Keen, M.C.R. Symons, J. Chem. Soc.N 8 (1962) 2873.

[33] M. Green, J. Linnett, Trans. Faraday Soc. 57 (1961) 1.

[34] R.M. Golding, M. Heuchman, J. Chem. Phys. 40 (1964) 1554.

[35] J. Tateno, K. Gesi, J. Chem. Phys. 40 (1964) 1317.

[36] N.M. Atherton, R.N. Doxon, G.H. Kirby, Trans. Faraday Soc. 60 (1964) 1688.

[37] V. Balzani, R. Ballardini, N. Sabbatini, L. Moggi, Inorg. Chem. 7 (1968) 1398.

[38] W.W. Wendlandt, J.H. Woodlock, J. Inorg. Nucl. Chem. 27 (1965) 259.

[39] S.A. Altshuler, B.M. Kozyrev, Electronic Paramagnetic Resonance of Compounds of Transient Groups, Nauka, Moscow, 1972.

[40] A. Treinin, E. Hayon, J. Am. Chem. Soc. 92 (1970) 5821.

[41] M. Anbar, J.K. Thomas, J. Phys. Chem. 68 (1964) 3829.

[42] M. Gratzel, A. Henglein, J. Lillis, G. Beck, Ber. Bunsenges. Phys. Chem. 73 (1969) 646.

[43] M. Ottolenghi, J. Rabani, J. Phys. Chem. 72 (1968) 593.

[44] M. Hoshino, Y. Nagashima, H. Seki, M. De Leo, P.C. Ford, Inorg. Chem. 37 (1998) 2464.